

Heat-resistant Pb(II)-based X-ray scintillating metal-organic frameworks for sensitive dosage detection via the aggregation-induced luminescent chromophore

Jian Lu,^{abc} Shuai-Hua Wang,^{ac} Yan Li,^d Wen-Fei Wang,^{ac} Cai Sun,^a Pei-Xin Li,^a Fa-Kun Zheng*^{ac} and Guo-Cong Guo*^a

^a *State Key Laboratory of Structural Chemistry, Fujian Institute of Research on the Structure of Matter, Chinese Academy of Sciences, Fuzhou, Fujian 350002, P. R. China.*

^b *University of Chinese Academy of Sciences, Beijing 100039, P.R. China.*

^c *Fujian Science & Technology Innovation Laboratory for Optoelectronic Information of China, Fuzhou, Fujian 350108, P. R. China.*

^d *Key Laboratory of Optoelectronic Materials Chemistry and Physics, Chinese Academy of Sciences, Fuzhou, Fujian 350002, P. R. China*

Methods

Caution! X-ray scintillation measurements are carried out on an updated FLS1000 instrument equipped with HAMAMATSU R928 photodetector where the excitation source is replaced with X-ray triggered by high purity tungsten target. In case of X-ray radiation against human body, suitable precautions must be followed for its processing.

Materials and Measurements

Caution! X-ray scintillation measurements are carried out on an updated FLS1000 instrument where the excitation source is replaced with X-ray triggered by high purity tungsten target. In case of X-ray radiation against human body, suitable precautions must be followed for its processing.

All reagents purchased commercially were used without further purification. Powdered X-ray diffraction patterns were collected on a Rigaku Miniflex 600 diffractometer using Cu K_{α} radiation ($\lambda = 1.5406 \text{ \AA}$) in the 2θ range of 5–65°. The simulated patterns were derived from the Mercury version 4.1.3 (<https://www.ccdc.cam.ac.uk/support-and-resources/downloads/>). The FT-IR spectra were obtained on a PerkinElmer Spectrum using KBr disks in the range of 4000–400 cm^{-1} . Thermogravimetric analysis (TGA) measurements and differential scanning calorimetry (DSC) measurements were done on METTLER TOLEDO instrument in N_2 with the sample heated in an Al_2O_3 crucible at a heating rate of 5 $^{\circ}\text{C}\cdot\text{min}^{-1}$. Elemental analyses of C, H and O were performed on an Elementar Vario EL III microanalyzer. UV-Vis absorption spectra were measured in the reflectance mode at room temperature on a Perkin-Elmer Lambda 900 UV/Vis/NIR spectrophotometer with an integrating sphere attachment and BaSO_4 as a reference. Photoluminescent spectra were recorded on a single-grating Edinburgh FL920 fluorescence spectrometer

equipped with a 450 W Xe lamp. Lifetimes were measured on an Edinburgh FLS1000 UV/Vis/NIR Fluorescence Spectrometer.

Temperature dependent PL spectra were collected using an Edinburgh FLS1000 UV/Vis/NIR Fluorescence Spectrometer equipped with a 30 mW, 365 nm laser, Corporation Horiba JobinYvon (France). The selected single crystal was put into the sample room (Linkam attachment, temperature range: 77–473 K. We first annealed the sample at 473 K for half an hour in order to obtain reliable temperature dependent PL spectral data. Then the temperature was decreased to 77 K and gradually was increased back to 473 K for PL recording. PL spectra data were collected after the temperature stabilized at a setting value for 5 min.

Room-temperature & 77K-low-temperature transient fluorescence was measured using a FLS920 full functional fluorescence spectrometer (Edinburgh Instruments, UK) equipped with a μ F 920 H (100 W) hydrogen lamp and a repetition frequency of 100 Hz.

X-ray crystallographic study

The intensity data sets were collected on Rigaku PILATUS CCD diffractometer with graphite-monochromated Cu K_{α} radiation ($\lambda = 0.71073 \text{ \AA}$) using the ω - 2θ scan technique and reduced by the *CrysAlisPro* software.¹ The structures were solved by the direct method and refined by full-matrix least squares on F^2 using the Olex2 1.2 software with anisotropic thermal parameters for all non-hydrogen atoms.² Hydrogen atoms were added geometrically and refined using the riding model. By using the program PLATON.³ Crystal data and structure refinement results for **Pb-SMOF-Cl** and **Pb-SMOF-Br** are summarized in **Tables S1–S3**.

Synthesis of $[\text{Pb}_2(2,6\text{-ndc})_{1.5}(\mu_3\text{-Br})]_n$ Pb-SMOF-Br. A mixture of 2,6- H_2ndc (64.86 mg, 0.3 mmol) and PbBr_2 (110.70 mg, 0.3 mmol) in DMA/ H_2O mixed solvent (6 mL, V/V 2:1) was sealed in a 25mL Teflon-lined stainless vessel under autogenous pressure, and treated with ultrasound for 30 mins, then heated at 100 °C, kept for 72 hrs and cooled to room temperature. Pale yellow block crystals of **Pb-SMOF-Br**

were formed, then collected and washed with DMA for three times, obtained in 63% yield after being dried under vacuum oven (based on 2,6-H₂ndc). Anal. calcd (%) for C₁₈H₉BrO₆Pb₂: C 26.51, H 1.11, O 11.77. Found (%): C 26.72, H 1.06, O 11.14. FT-IR (KBr pellet, cm⁻¹): 3051w, 1597m, 1533s, 1484s, 1411s, 1330s, 1199m, 929m, 841w, 790s, 542m, 443m.

Synthesis of [Pb₂(2,6-ndc)_{1.5}(μ₂-Cl)]_n Pb-SMOF-Cl. The compound is synthesized according to the reported literature.⁴ Similar with that of **Pb-SMOF-Br**, except that 83.44 mg (0.3 mmol) PbCl₂ were added for the substitution of PbBr₂ in the reaction.

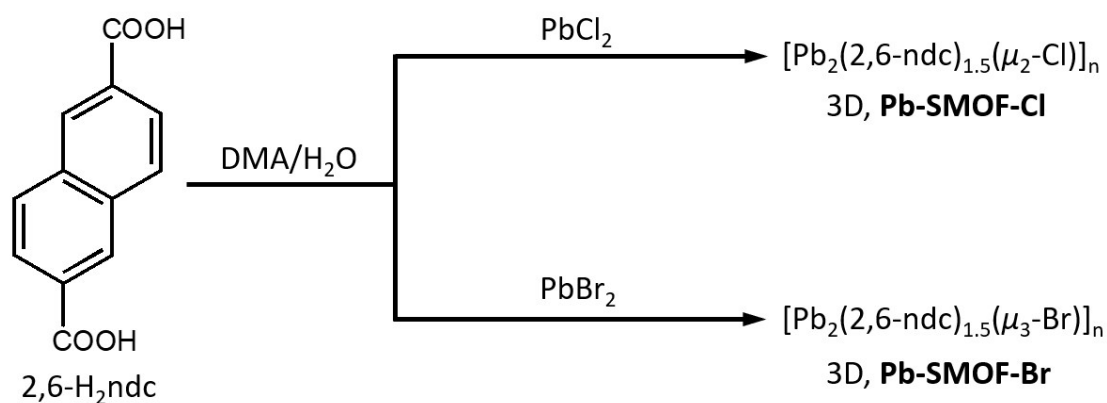
Calculations of Intermolecular Interactions

To obtain plots of the electron density ($\rho(r)$) and reduced density gradient ($s = 1/(2(3\pi^2)^{1/3})|\nabla\rho(r)|/\rho(r)^{4/3}$), density-functional theory (DFT) calculations were performed for a selected set of **Pb-SMOF-Cl** and **Pb-SMOF-Br**. Calculations were performed with B3LYP functional⁵ and the 6-31G* basis set for C, H, O and SDD basis set for Cl, Br and Pb using the Gaussian 09 program.⁶ The results were analyzed by Multiwfn software.⁷

Calculations of electronic structures and density of states (DOS)

The calculation models for **Pb-SMOF-Cl** and **Pb-SMOF-Br** were built directly from their single-crystal X-ray diffraction data. The electronic structure calculations based on DFT were performed using the CASTEP package.⁸ The exchange-correlation energy was described by the revised Perdew-Burke-Eruzerhof (RPBE) function within the generalized gradient approximation (GGA).⁹ The norm conserving pseudopotentials were chosen to modulate the electron-ion interaction.¹⁰ The orbital electrons of C 2s²2p², H 1s¹, O 2s²2p⁴, Cl 3s²3p⁵, Br 4s²4p⁵ and Pb 6s²6p² were treated as valence electrons. The plane-

wave cut-off energy was 830 eV, and the threshold of 5×10^{-7} eV was set for the self-consistent field convergence of the total electronic energy. The numerical integration of the Brillouin zone was performed using $4 \times 1 \times 2$ and $4 \times 2 \times 1$ Monkhorst–Pack k -point meshes for **Pb-SMOF-Cl** and **Pb-SMOF-Br**, respectively. The Fermi level was selected as the reference and set at 0.00 eV by default.



Scheme S1. The synthetic routines of **Pb-SMOF-Cl** and **Pb-SMOF-Br** under 100 °C through solvothermal reactions.

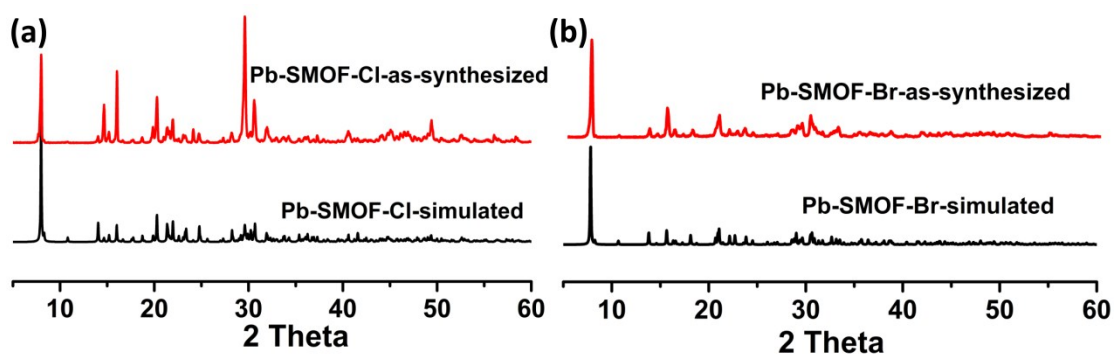


Fig. S1 The powdered X-ray diffraction (PXRD) patterns of **Pb-SMOF-Cl** (a) and **Pb-SMOF-Br** (b).

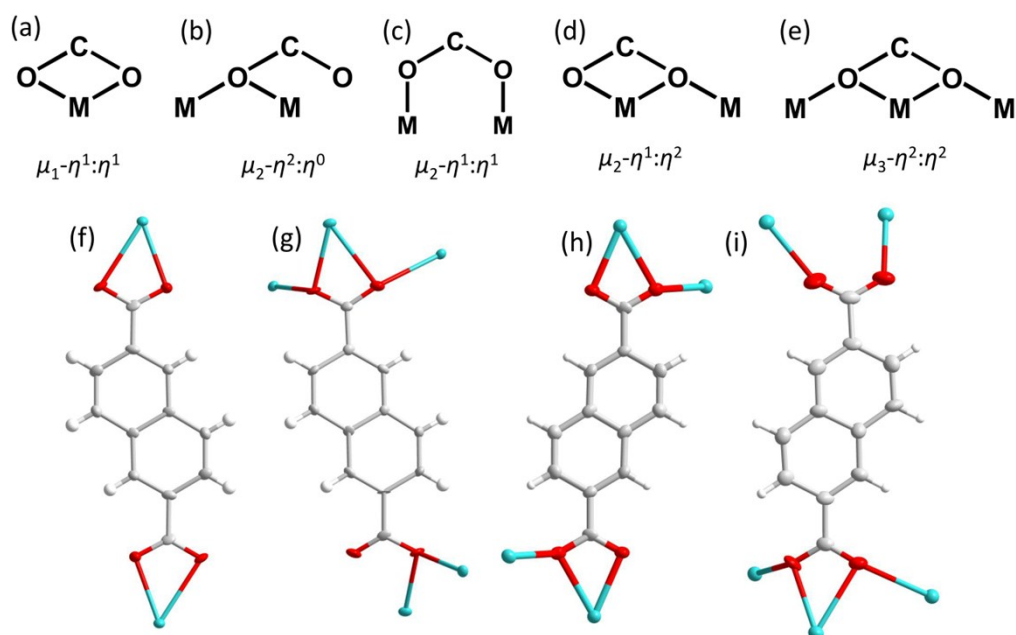


Fig. S2 The coordination modes of carboxylate group with Pb^{2+} (a–e), and the bridging μ_2 mode of $2,6\text{-ndc}^{2-}$ in **Pb-SMOF-Cl** (f), μ_5 mode of $2,6\text{-ndc}^{2-}$ in **Pb-SMOF-Cl** (g), μ_4 mode of $2,6\text{-ndc}^{2-}$ in **Pb-SMOF-Br** (h) and μ_5 mode of $2,6\text{-ndc}^{2-}$ in **Pb-SMOF-Br** (i).

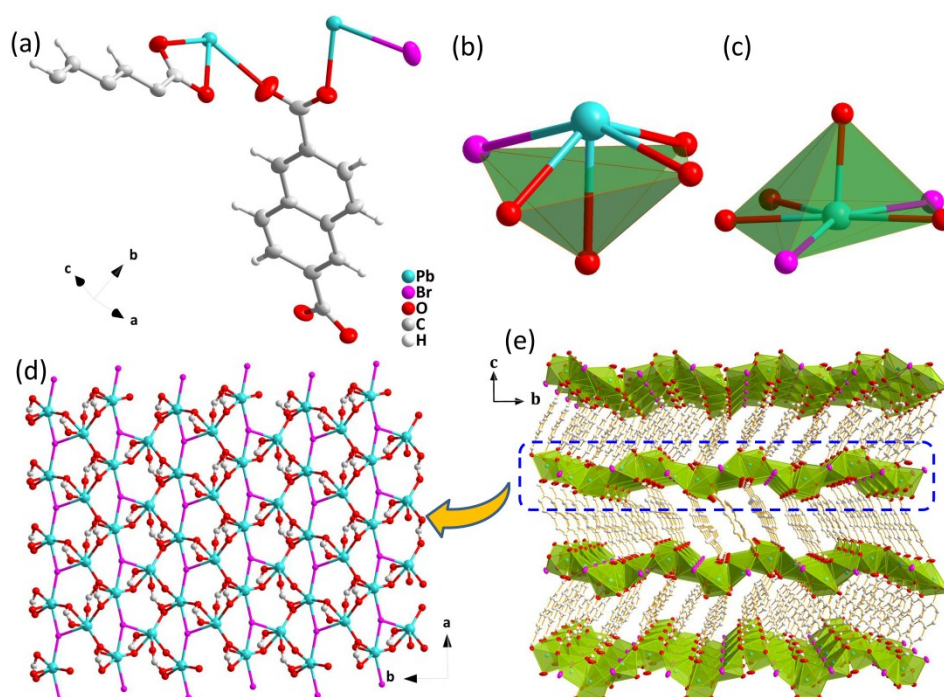


Fig. S3 For **Pb-SMOF-Br**: (a) the asymmetric unit, (b) the hemi-directed coordination sphere of Pb1 , (c) the holo-directed coordination sphere of Pb2 , (d) the Pb-O-Br layer parallel to the ab plane, and (e) the 3D framework.

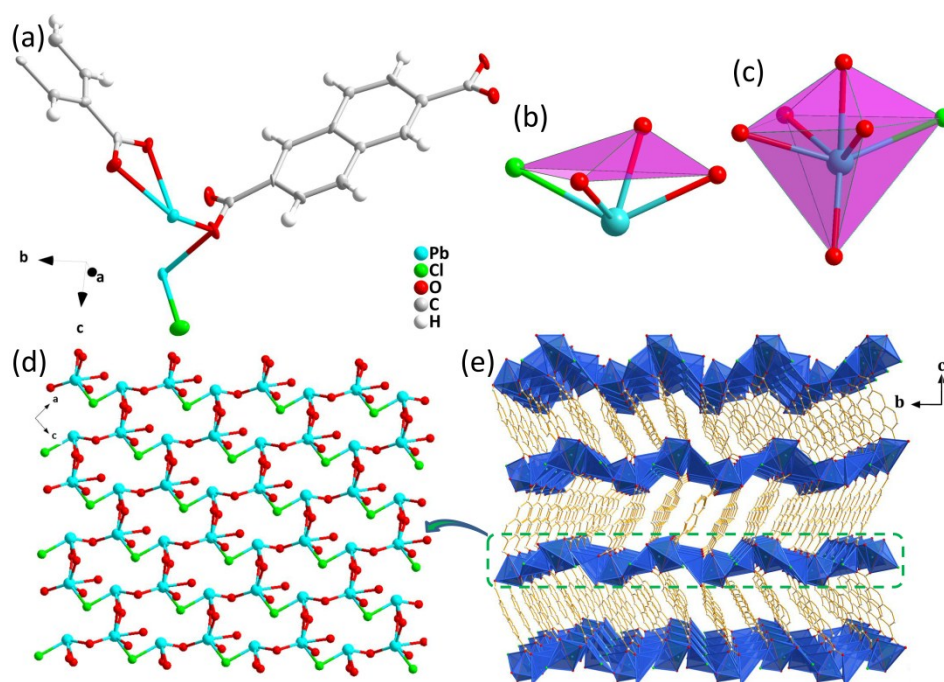


Fig. S4 For **Pb-SMOF-Cl**: (a) the asymmetric unit, (b) the hemi-directed coordination sphere of Pb1, (c) the holo-directed coordination sphere of Pb2, (d) the Pb–O–Cl layer parallel to the *ac* plane, and (e) the 3D framework.

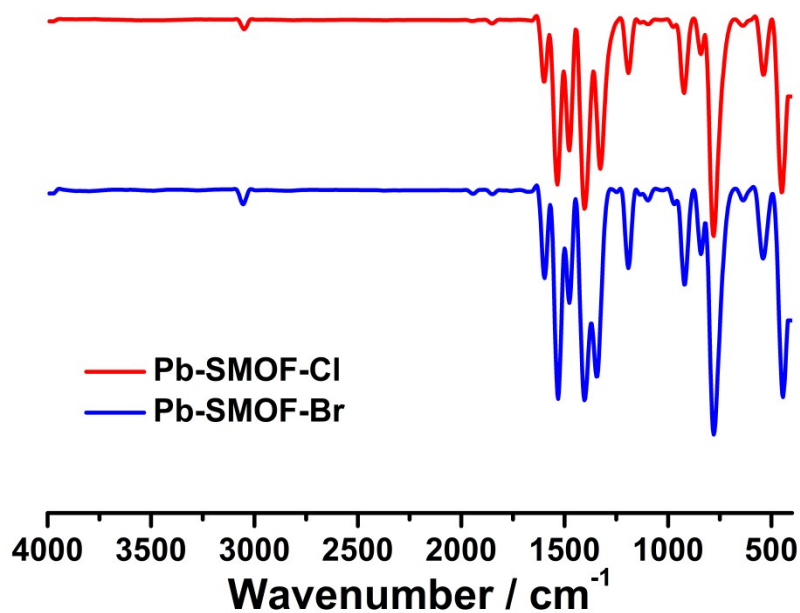


Fig. S5 The FT-IR curves of **Pb-SMOF-Cl** (red) and **Pb-SMOF-Br** (blue).

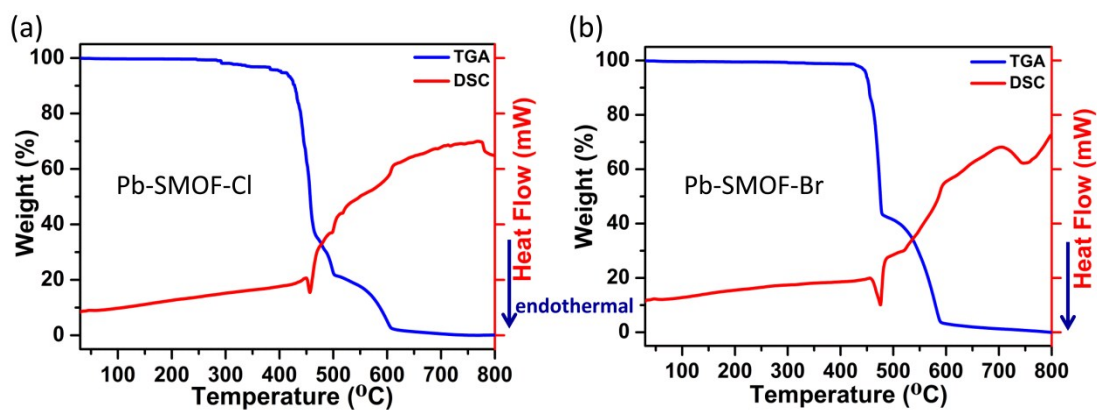


Fig. S6 The TG&DSC curves of (a) **Pb-SMOF-Cl** and (b) **Pb-SMOF-Br**.

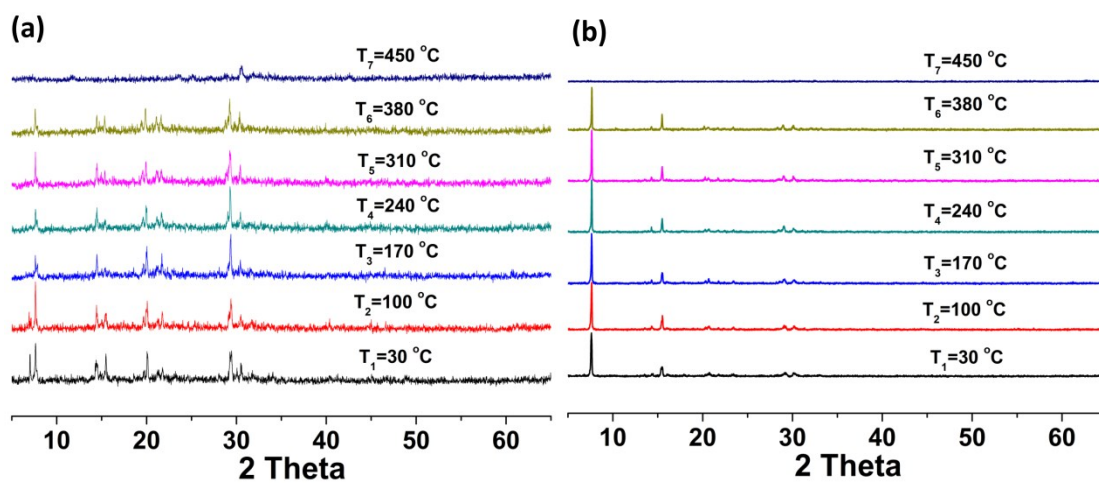


Fig. S7 The variable-temperature PXRD patterns from 30 to 450 °C of **Pb-SMOF-Cl** (a) and **Pb-SMOF-Br** (b).

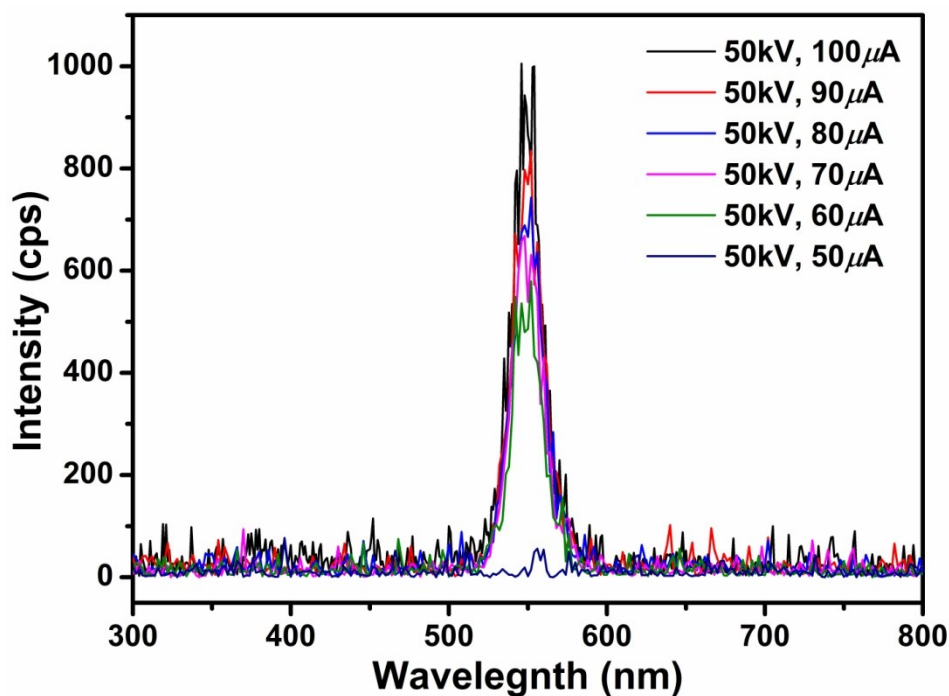


Fig. S8 The XSL signals of (a) powdered CsPbBr₃ under exposure of X-ray tube with voltage fixed at 50 kV, current ranging from 100 to 50 μ A.

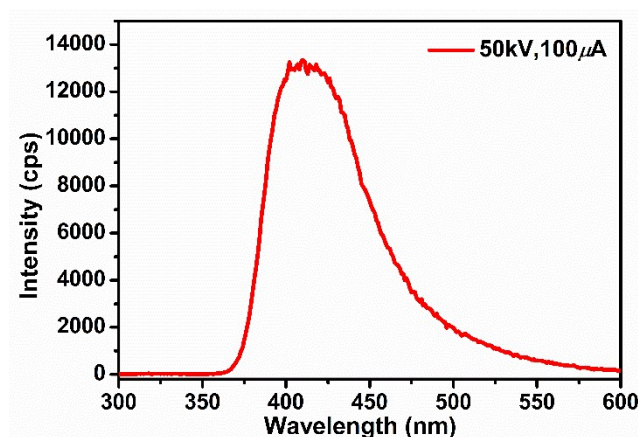


Fig. S9 The XSL spectra of the commercial powdered crystalline LYSO:Ce with the X-ray tube voltage of 50 kV and the tube current of 100 μ A.

Notes: The scintillation intensity of powdered crystalline LYSO:Ce is about \sim 10 times higher than that of **Pb-SMOFs** under the same experimental condition (Fig. S8, Fig. 2).

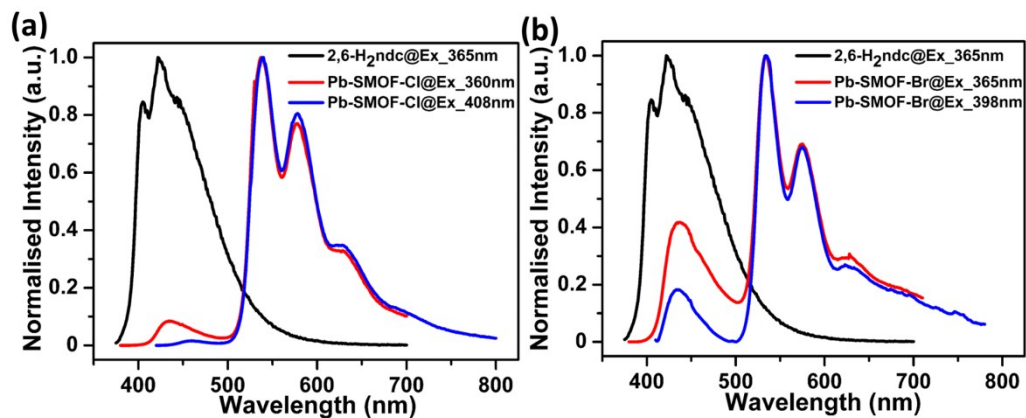


Fig. S10 The emission spectra of free ligand 2,6-H₂ndc and (a) **Pb-SMOF-Cl**, and (b) **Pb-SMOF-Br**.

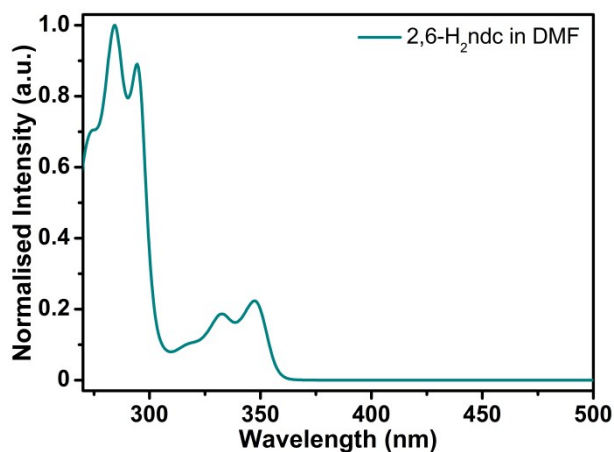


Fig. S11 The liquid UV-Vis absorption spectrum of 2,6-H₂ndc in dilute DMF solution (10⁻⁵ mol/L).

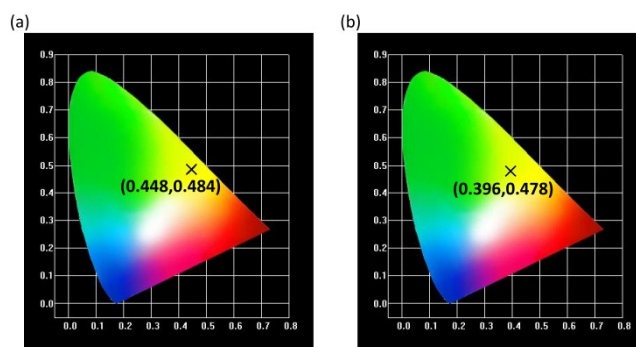


Fig. S12 Photoluminescent CIE profiles of (a) **Pb-SMOF-Cl** and (b) **Pb-SMOF-Br**.

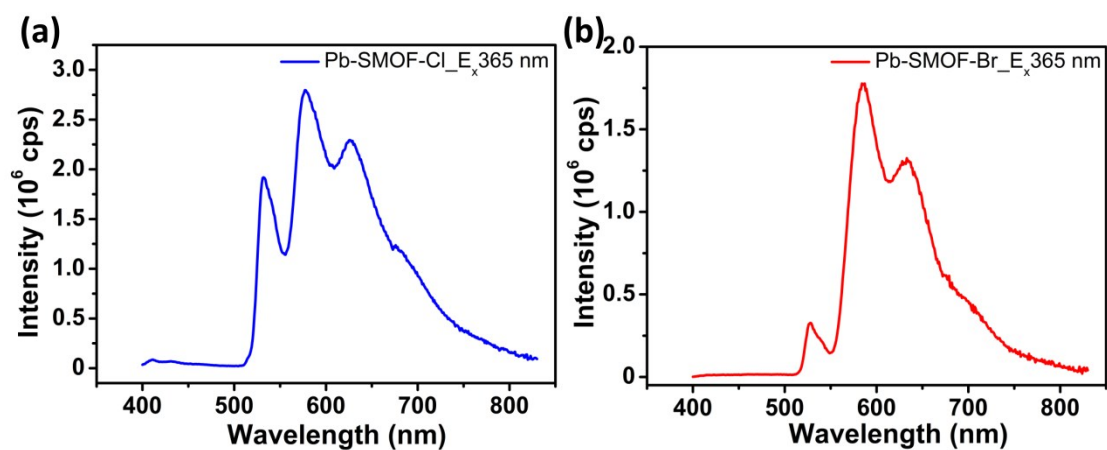


Fig. S13 The photoluminescent (PL) spectra of **Pb-SMOF-Cl** and **Pb-SMOF-Br** upon excitation of 365 nm at ~ 77 K.

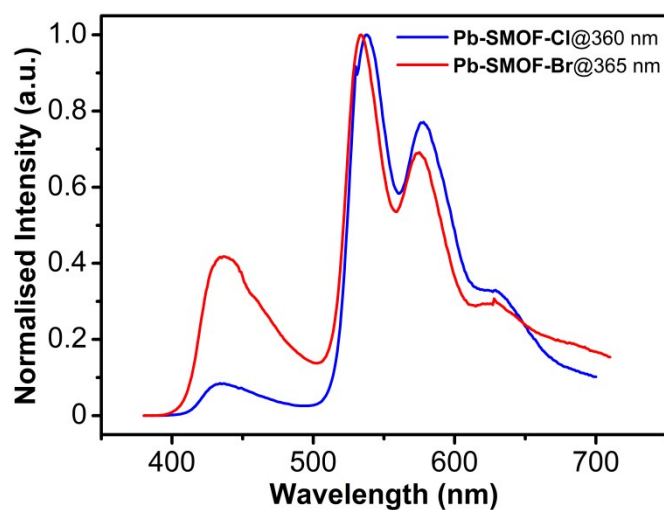


Fig. S14 The ambient PL spectra of **Pb-SMOFs** after a exposure under 473 K for 2 hours.

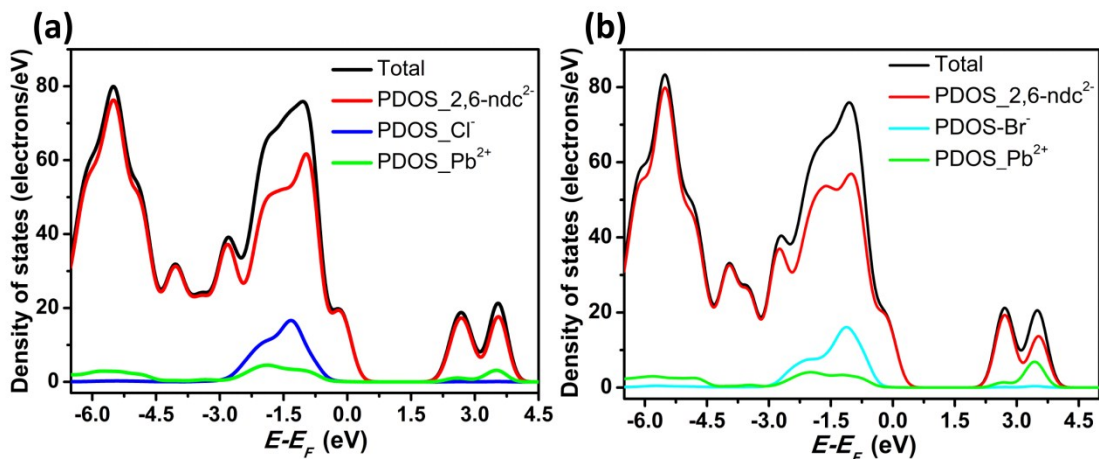


Fig. S15 Profiles of the total/partial electronic density of state of (a) **Pb-SMOF-Cl** and (b) **Pb-SMOF-Br**.

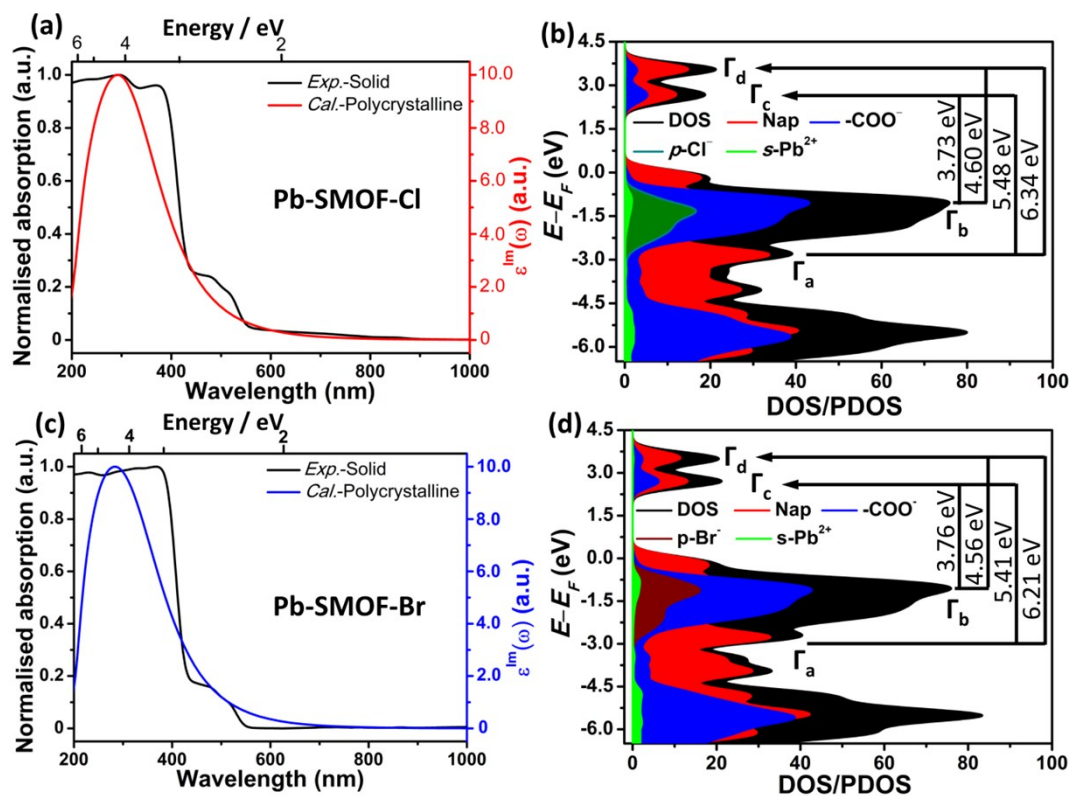


Fig. S16 The normalised experimental solid-state UV-Vis absorption spectra and the imaginary part curve of calculated dielectric constants of (a) **Pb-SMOF-Cl** and (c) **Pb-SMOF-Br**, and total and partial DOS of (b) **Pb-SMOF-Cl** and (d) **Pb-SMOF-Br**. The Fermi level (E_F) is set to zero by default. Nap means naphthalene nucleus, and COO^- means carboxylate group.

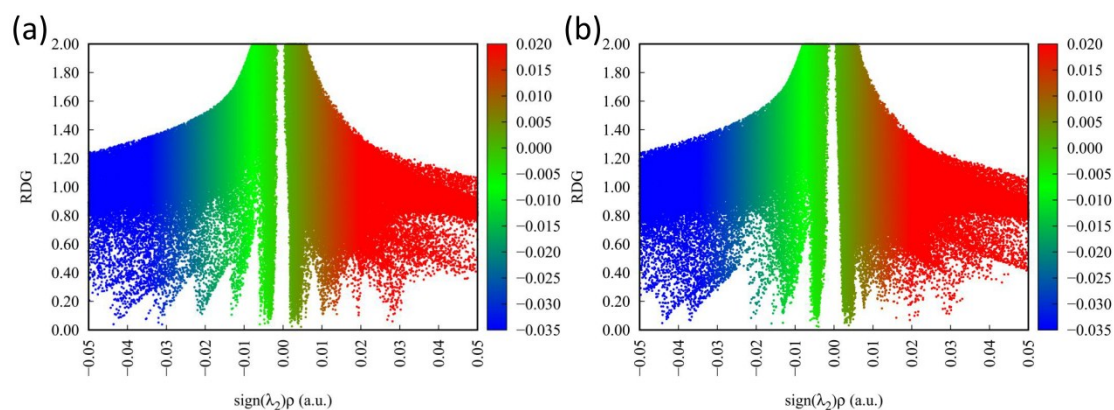


Fig. S17 Plots of the reduced density gradient (RDG) *versus* the electron density (ρ) multiplied by the sign of λ_2 for (a) **Pb-SMOF-Cl** and (b) **Pb-SMOF-Br**. The surfaces are colored on blue-green-red scale according to values of $\text{sign}(\lambda_2)\rho$, ranging from -0.05 to 0.05 a.u. Blue indicates strong attractive interactions and red indicates strong nonbonded overlap.

Table S1 Crystal data and structure refinement parameters for **Pb-SMOF-Cl** and **Pb-SMOF-Br**.

Crystal data	Pb-SMOF-Cl	Pb-SMOF-Br
CCDC number	1950799	1950800
Empirical formula	$\text{C}_{18}\text{H}_9\text{ClO}_6\text{Pb}_2$	$\text{C}_{18}\text{H}_9\text{BrO}_6\text{Pb}_2$
Formula weight	771.08	815.54
Temperature	293(2)	293(2)
Wavelength (\AA) / $\text{MoK}\alpha$	0.71073	0.71073
Crystal system	monoclinic	monoclinic
Space group	$P2_1/c$	$P2_1/c$
a (\AA)	6.0559(3)	6.0493(4)
b (\AA)	22.1208(11)	12.1823(6)
c (\AA)	12.1647(6)	22.6741(14)
α ($^\circ$)	90	90
β ($^\circ$)	94.721(5)	91.064(5)
γ ($^\circ$)	90	90

Electronical Supporting Information

V (Å ³)	1624.07(14)	1670.67(17)
Z	4	4
<i>Calcd.</i> density (g cm ⁻³)	3.154	3.242
Absorption coefficient (mm ⁻¹)	20.907	22.556
$F(000)$	1384	1456
2θ range	6.97 to 54.98	7.19 to 55.00
Reflections collected	13385	23788
Completeness to $\theta = 27.49^\circ$	96.8%	99.0%
Data/restraints/parameters	3603/12/245	3803/0/244
Goodness-of-fit on F^2	1.060	1.165
Final R indices [$I > 2\sigma(I)$]	$R_1 = 0.0315$ $wR_2 = 0.0667$	$R_1 = 0.0522$ $wR_2 = 0.0903$

$${}^a R_1 = \sum(F_o - F_c)/\sum F_o, {}^b wR_2 = [\sum w(F_o^2 - F_c^2)^2/\sum w(F_o^2)^2]^{1/2}.$$

Table S2 Selected bond lengths (Å) and bond angles (°) in **Pb-SMOF-Cl** and **Pb-SMOF-Br**.

<u>Pb-SMOF-Cl</u>			
Pb(1)–O(5)#1	2.414(4)	Pb(2)–O(5)#1	2.731(5)
Pb(1)–O(6)#1	2.710(4)	Pb(2)–O(6)#3	2.687(4)
Pb(1)–O(1)	2.355(5)	Pb(2)–O(1)	2.677(5)
Pb(1)–Cl(1)	2.8921(18)	Pb(2)–O(4)	2.392(4)
Pb(2)–O(3)	2.605(4)	Pb(2)–Cl(1)#2	2.9173(18)
O(5)#1–Pb(1)–Cl(1)	76.02(11)	O(5)#1–Pb(2)–Cl(1)#2	142.11(10)
O(5)#1–Pb(1)–O(6)#1	50.60(14)	O(6)#3–Pb(2)–Cl(1)#2	120.17(11)
O(6)#1–Pb(1)–Cl(1)	126.46(10)	O(6)#3–Pb(2)–O(5)#1	92.24(14)
O(1)–Pb(1)–Cl(1)	76.54(12)	O(1)–Pb(2)–Cl(1)#2	96.40(10)
O(1)–Pb(1)–O(5)	79.23(15)	O(1)–Pb(2)–O(5)#1	68.42(13)
O(1)–Pb(1)–O(6)#1	95.10(16)	O(1)–Pb(2)–O(6)#3	134.71(14)
O(3)–Pb(2)–Cl(1)#2	71.29(10)	O(4)–Pb(2)–Cl(1)#2	81.96(12)
O(3)–Pb(2)–O(5)#1	71.81(13)	O(4)–Pb(2)–O(3)	52.57(14)
O(3)–Pb(2)–O(6)#3	134.73(13)	O(4)–Pb(2)–O(5)#1	82.56(15)
O(3)–Pb(2)–O(1)	79.28(14)	O(4)–Pb(2)–O(6)#3	84.14(14)
		O(4)–Pb(2)–O(1)	129.88(15)
<u>Pb-SMOF-Br</u>			
Pb(1)–O(6)	2.411(8)	Pb(2)–O(5)#4	2.687(8)
Pb(1)–O(5)	2.522(8)	Pb(2)–O(4)#2	2.631(8)
Pb(1)–O(3)#2	2.532(8)	Pb(2)–O(3) #2	2.549(8)

Electronical Supporting Information

Pb(1)–O(1)	2.470(10)	Pb(2)–O(2)	2.335(9)
Pb(1)–Br(1)#1	3.1179(14)	Pb(2)–Br(1)	3.0991(10)
		Pb(2)–Br(1)#3	3.0972(14)
O(6)–Pb(1)–Br(1)#1	80.1 (2)	O(5)#4–Pb(2)–Br(1)	71.71(16)
O(6)–Pb(1)–O(5)	53.2(3)	O(4)#2–Pb(2)–Br(1)	80.78(19)
O(6)–Pb(1)–O(3)#3	84.8(3)	O(4)#2–Pb(2)–Br(1)#3	121.38(19)
O(6)–Pb(1)–O(1)	127.0(4)	O(4)#2–Pb(2)–O(5) #4	152.2(3)
O(5)–Pb(1)–Br(1)#1	73.43 (18)	O(3)#2–Pb(2)–Br(1)	130.95(17)
O(5)–Pb(1)–O(3)#2	75.0 (3)	O(3)#2–Pb(2)–Br(1)#3	71.41(17)
O(3)–Pb(1)–Br(1)#1	148.08(18)	O(3)#2–Pb(2)–O(5) #4	157.3(2)
O(1)–Pb(1)–Br(1)#1	83.7(3)	O(3)#2–Pb(2)–O(4)#2	50.4(3)
O(1)–Pb(1)–O(5)	73.8(4)	O(2)–Pb(2)–Br(1)#3	109.0(3)
O(1)–Pb(1)–O(3) #2	83.3(3)	O(2)–Pb(2)–Br(1)	82.9(3)
Br(1)#3–Pb(2)–Br(1)	154.99(5)	O(2)–Pb(2)–O(5)#4	88.6(3)
O(5)#4–Pb(2)–Br(1)#3	86.31(16)	O(2)–Pb(2)–O(4)#2	84.2(3)
		O(2)–Pb(2)–O(3)#2	94.6(3)

Symmetric codes:

For **Pb-SMOF-Cl**, #1 $1 - x, 1/2 + y, 1/2 - z$; #2 $x, 3/2 - y, -1/2 + z$; #3 $2 - x, 1/2 + y, 1/2 - z$;

For **Pb-SMOF-Br**, #1 $1 - x, -1/2 + y, 3/2 - z$; #2 $x, 1/2 - y, 1/2 + z$; #3 $-1 + x, y, z$; #4 $1 - x, 1/2 + y, 3/2 - z$.

Table S3 The geometrical parameters of π – π interactions between aromatic rings in **Pb-SMOF-Cl** and **Pb-SMOF-Br** calculated by the PLATON software.³

Cg(I)–Cg(J)	Cg–Cg(Å)	Alpha(°)	Beta(°)	Gamma(°)	CgI_Perp(Å)	CgJ_Perp(Å)	Slippage(Å)
Pb-SMOF-Cl							
Cg1–Cg3	3.718(4)	1.3(3)	22.8	22.4	3.437(3)	3.429(3)	1.439
Cg1–Cg3	3.664(4)	1.3(3)	19.2	20.3	–3.437(3)	3.461(3)	1.202
Cg1–Cg4	3.664(4)	1.3(3)	19.2	20.3	3.437(3)	3.461(3)	1.202
Cg1–Cg4	3.718(4)	1.3(3)	22.8	22.4	–3.437(3)	3.429(3)	1.439
Cg2–Cg2	3.800(4)	0.0(3)	26.8	26.8	–3.391(3)	–3.391(3)	1.715
Cg2–Cg3	3.756(4)	5.1(3)	25.5	27.8	3.322(3)	3.390(3)	1.618
Cg2–Cg4	3.756(4)	5.1(3)	25.5	27.8	–3.322(3)	3.390(3)	1.618
Cg3–Cg1	3.718(4)	1.3(3)	22.4	22.8	3.428(3)	3.436(3)	1.419
Cg3–Cg1	3.664(4)	1.3(3)	20.3	19.2	3.461(3)	–3.436(3)	1.270
Cg3–Cg2	3.755(4)	5.1(3)	27.8	25.5	3.389(3)	3.322(3)	1.751
Cg4–Cg1	3.664(4)	1.3(3)	20.3	19.2	3.461(3)	3.436(3)	1.270
Cg4–Cg1	3.718(4)	1.3(3)	22.4	22.8	3.428(3)	–3.436(3)	1.419
Cg4–Cg2	3.755(4)	5.1(3)	27.8	25.5	3.390(3)	–3.322(3)	1.751
Pb-SMOF-Br							
Cg6–Cg8	3.649(7)	1.1(6)	20.5	20.8	–3.411(5)	3.419(5)	1.278
Cg6–Cg8	3.762(7)	1.1(6)	24.3	25.0	3.409(5)	3.431(5)	1.545

Electronical Supporting Information

Cg6-Cg9	3.762(7)	1.1(6)	24.3	25.0	-3.409(5)	3.431(5)	1.545
Cg6-Cg9	3.649(7)	1.1(6)	20.5	20.8	3.411(5)	3.419(5)	1.278
Cg7-Cg7	3.703(7)	0.0(6)	26.9	26.9	-3.303(5)	-3.302(5)	1.677
Cg7-Cg8	3.792(7)	3.8(5)	25.8	28.4	3.365(5)	3.412(5)	1.653
Cg7-Cg9	3.792(7)	3.8(5)	25.8	28.4	-3.365(5)	-3.412(5)	1.653
Cg8-Cg6	3.651(7)	1.1(6)	20.8	20.5	3.419(5)	-3.412(5)	1.298
Cg8-Cg6	3.763(7)	1.1(6)	25.0	24.3	3.430(5)	3.410(5)	1.590
Cg8-Cg7	3.791(7)	3.8(5)	28.4	25.8	3.411(5)	3.336(5)	1.801
Cg9-Cg6	3.762(7)	1.1(6)	25.0	24.3	3.430(5)	-3.410(5)	1.590
Cg9-Cg6	3.651(7)	1.1(6)	20.8	20.5	3.419(5)	3.412(5)	1.298
Cg9-Cg7	3.791(7)	3.8(5)	28.4	25.8	3.411(5)	-3.336(5)	1.801

Notes: Cg(I) / Cg(J) = the plane of the ring in the structure, Alpha = dihedral angle between planes of ring I and J ($^{\circ}$), Beta = angle Cg(I)-Cg(J) or Cg(I)-->Me vector and normal to plane I ($^{\circ}$), Gamma = angle Cg(I)- Cg(J) vector and normal to plane J ($^{\circ}$), Cg-Cg = distance between ring centroids (\AA), CgI_Perp = perpendicular distance of Cg(I) on ring J (\AA), CgJ_Perp = perpendicular distance of Cg(J) on ring I ($^{\circ}$), Slippage = distance between Cg(I) and perpendicular projection of Cg(J) on ring I ($^{\circ}$).

Electronical Supporting Information

Table S4 Calculation results of the effective atomic number (Z_{eff}) values of **Pb-SMOFs** and **CsPbBr₃**.

	Pb-SMOF-Cl	Pb-SMOF-Br	CsPbBr₃
Compound	C ₁₈ H ₉ ClO ₆ Pb ₂	C ₁₈ H ₉ BrO ₆ Pb ₂	CsPbBr ₃
Pb content	53.74%	50.81%	35.70%
Z_{eff}	70.2	69.3	65.9

Notes: In the approximation of dominance of photoelectric effect for X-rays and of the atomic mass in proportion to Z , the Z_{eff} value for a compound consisting of $A_xB_yC_z$ can be given by the following equation:¹¹

$$Z_{eff} = [(xM_aZ_a^4 + yM_bZ_b^4 + zM_cZ_c^4)/(xM_a + yM_b + zM_c)]^{1/4}$$

where M_a , M_b and M_c are the atomic masses of A, B and C, respectively; Z_a , Z_b and Z_c are atomic numbers of A, B and C, respectively.

Determination of the Z_{eff} value for compound **Pb-SMOF-Cl** (C₁₈H₉ClO₆Pb₂):

$$Z_{eff} = [(18 \times 12.01 \times 6^4 + 9 \times 1.008 \times 1^4 + 1 \times 35.45 \times 17^4 + 6 \times 16.00 \times 8^4 + 2 \times 207.2 \times 82^4)/(18 \times 12.01 + 9 \times 1.008 + 1 \times 35.45 + 6 \times 16.00 + 2 \times 207.2)]^{1/4} = 70.2$$

Determination of the Z_{eff} value for compound **Pb-SMOF-Br** (C₁₈H₉BrO₆Pb₂):

$$Z_{eff} = [(18 \times 12.01 \times 6^4 + 9 \times 1.008 \times 1^4 + 1 \times 79.90 \times 35^4 + 6 \times 16.00 \times 8^4 + 2 \times 207.2 \times 82^4)/(18 \times 12.01 + 9 \times 1.008 + 1 \times 79.90 + 6 \times 16.00 + 2 \times 207.2)]^{1/4} = 69.3$$

Determination of the Z_{eff} value for compound **CsPbBr₃**:

$$Z_{eff} = [(1 \times 132.9 \times 55^4 + 1 \times 207.2 \times 82^4 + 3 \times 79.90 \times 35^4)/(1 \times 132.9 + 1 \times 207.2 + 3 \times 79.90)]^{1/4} = 65.9$$

Electronical Supporting Information

Table S5 Fluorescence decay parameters of **Pb-SMOF-Cl** and **Pb-SMOF-Br** at 298 K.

$\lambda_{\text{em}} / \text{nm}$	τ_1	$A_1 (\%)$	τ_2	$A_2 (\%)$	τ_3	$A_3 (\%)$	τ
Pb-SMOF-Cl							
437	0.78 (ns)	31.43	5.08 (ns)	20.80	28.98 (ns)	47.77	14.37 (ns)
538	7.78 (μs)	19.77	24.61 (μs)	59.93	82.80 (μs)	20.30	32.95 (μs)
578	7.94 (μs)	18.65	23.75 (μs)	58.84	80.36 (μs)	22.51	33.55 (μs)
630	7.49 (μs)	17.25	23.17 (μs)	53.72	91.56 (μs)	29.04	47.15 (μs)
Pb-SMOF-Br							
437	4.55 (ns)	10.53	29.57 (ns)	89.47			26.89 (ns)
534	5.84 (μs)	34.26	22.28 (μs)	65.74			15.96 (μs)
575	6.83 (μs)	38.74	23.57 (μs)	61.26			16.06 (μs)
630	8.83 (μs)	58.24	35.76 (μs)	41.76			17.08 (μs)

Table S6 Fluorescence decay parameters of **Pb-SMOF-Cl** and **Pb-SMOF-Br** at 77 K.

$\lambda_{\text{em}} / \text{nm}$	τ_1	$A_1 (\%)$	τ_2	$A_2 (\%)$	τ_3	$A_3 (\%)$	T
Pb-SMOF-Cl							
431	0.23 (ns)	85.21	15.42 (ns)	14.79			2.31 (ns)
532	31.83 (μs)	44.57	188.2 (μs)	55.43			112.18 (μs)
578	69.13 (μs)	50.89	530.4 (μs)	49.11			277.76 (μs)
627	119.1 (μs)	36.88	860.4 (μs)	63.12			570.72 (μs)
Pb-SMOF-Br							
436	5.63 (ns)	22.56	35.69 (ns)	77.44			28.62 (ns)
528	15.29 (μs)	37.06	65.15 (μs)	62.94			44.57 (μs)
586	204.0 (μs)	22.00	1489 (μs)	78.00			1196.43 (μs)
633	386.5 (μs)	36.53	1586 (μs)	63.47			1096.25 (μs)

Reference

1. CrysAlisPro, Agilent Technologies, Version 1. 171. 37. 33, 2014.
2. O.V. Dolomanov, L.J. Bourhis, R.J. Gildea, J.A.K. Howard, H. Puschmann, *J. Appl. Cryst.*, 2009, **42**, 339–341.
3. A. L. Spek, *J. Appl. Crystallogr.*, 2003, **36**, 7–13.
4. J. Lu, X.-H. Xin, Y.-J. Lin, S.-H. Wang, J.-G. Xu, F.-K. Zheng and G.-C. Guo, *Dalton Trans.*, 2019, **48**, 1722–1731.

5. C. T. Lee, W. T. Yang, R. G. Parr, *Phys. Rev. B: Condens. Matter Mater. Phys.*, 1988, **37**, 785–789
6. M. J. Frisch, G. W. Trucks, H. B. Schlegel, G. E. Scuseria, M. A. Robb, J. R. Cheeseman, G. Scalmani, V. Barone, B. Mennucci, G. A. Petersson, H. Nakatsuji, M. Caricato, X. Li, H. P. Hratchian, A. F. Izmaylov, J. Bloino, G. Zheng, J. L. Sonnenberg, M. Hada, M. Ehara, K. Toyota, R. Fukuda, J. Hasegawa, M. Ishida, T. Nakajima, Y. Honda, O. Kitao, H. Nakai, T. Vreven, J. A. Montgomery Jr., J. E. Peralta, F. Ogliaro, M. Bearpark, J. J. Heyd, E. Brothers, K. N. Kudin, V. N. Staroverov, R. Kobayashi, J. Normand, K. Raghavachari, A. Rendell, J. C. Burant, S. S. Iyengar, J. Tomasi, M. Cossi, N. Rega, J. M. Millam, M. Klene, J. E. Knox, J. B. Cross, V. Bakken, C. Adamo, J. Jaramillo, R. Gomperts, R. E. Stratmann, O. Yazyev, A. J. Austin, R. Cammi, C. Pomelli, J. W. Ochterski, R. L. Martin, K. Morokuma, V. G. Zakrzewski, G. A. Voth, P. Salvador, J. J. Dannenberg, S. Dapprich, A. D. Daniels, Ö. Farkas, J. B. Foresman, J. V. Ortiz, J. Cioslowski and D. J. Fox, Gaussian 09 Revision D.01, Gaussian, Inc., Wallingford CT, 2009.
7. T. Lu, F.-W. Chen, *J. Comput. Chem.*, 2012, **33**, 580–592.
8. S.-J. Clark, M.-D. Segall, C.-J. Pickard, P.-J. Hasnip, M.-I. J. Probert, K. Refson and M.-C. Payne, *Z. Kristallogr. – Cryst. Mater.*, 2005, **220**, 567–570.
9. (a) B. Hammer, L. B. Hansen, J. K. Norskov, *Phys. Rev. B: Condens. Matter Mater. Phys.*, 1999, **59**, 7413–7421; (b) J. P. Perdew, Y. Wang, *Rev. B: Condens. Matter Mater. Phys.*, 1992, **45**, 13244–13249.
10. (a) D. R. Hamann, M. Schlüter, C. Chiang, *Phys. Rev. Lett.*, 1979, **43**, 1494–1497; (b) J. S. Lin, A. Qteish, M. C. Payne, V. Heine, *Phys. Rev. B: Condens. Matter Mater. Phys.*, 1993, **47**, 4174–4180.
11. M. Ishii and M. Kobayashi, *Prog. Crystal Growth and Charact.*, 1991, **23**, 245–311.